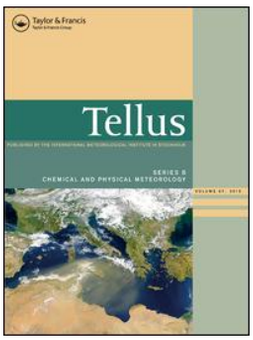

Tellus B: Chemical and Physical Meteorology

ISSN: (Print) 1600-0889 (Online) Journal homepage: http://www.tandfonline.com/loi/zelb20

Aerosol physical properties and processes in the lower marine boundary layer: a comparison of shipboard sub-micron data from ACE-1 and ACE-2

Timothy S. Bates, Patricia K. Quinn, David S. Covert, Derek J. Coffman, James E. Johnson & Alfred Wiedensohler

To cite this article: Timothy S. Bates, Patricia K. Quinn, David S. Covert, Derek J. Coffman, James E. Johnson & Alfred Wiedensohler (2000) Aerosol physical properties and processes in the lower marine boundary layer: a comparison of shipboard sub-micron data from ACE-1 and ACE-2, Tellus B: Chemical and Physical Meteorology, 52:2, 258-272, DOI: 10.3402/tellusb.v52i2.16104

To link to this article: https://doi.org/10.3402/tellusb.v52i2.16104

Published online: 15 Dec 2016.

Tellus (2000), 52B, 258–272
Printed in UK. All rights reserved

TELLUS
ISSN 0280–6509

Aerosol physical properties and processes in the lower marine boundary layer: a comparison of shipboard sub-micron data from ACE-1 and ACE-2

By TIMOTHY S. BATES*[1,2,3] PATRICIA K. QUINN[1,2], DAVID S. COVERT[2,3], DEREK J. COFFMAN[1,2], JAMES E. JOHNSON[1,2] and ALFRED WIEDENSOHLER[4], [1]*NOAA/Pacific Marine Environmental Laboratory (PMEL), 7600 Sand Point Way NE, Seattle, Washington, 98115, USA;* [2]*The Joint Institute for the Study of the Atmosphere and Ocean (JISAO), University of Washington, Seattle, Washington, USA;* [3]*Department of Atmospheric Sciences, University of Washington, Seattle, Washington, USA;* [4]*Institute for Tropospheric Research, Leipzig, Germany*

(Manuscript received 28 January 1999; in final form 23 September 1999)

ABSTRACT

The goals of the IGAC Aerosol Characterization Experiments (ACE) are to determine and understand the properties and controlling processes of the aerosol in a globally representative range of natural and anthropogenically perturbed environments. ACE-1 was conducted in the remote marine atmosphere south of Australia while ACE-2 was conducted in the anthropogenically modified atmosphere of the Eastern North Atlantic. In-situ shipboard measurements from the RV *Discoverer* (ACE-1) and the RV *Professor Vodyanitskiy* (ACE-2), combined with calculated back trajectories can be used to define the physical properties of the sub-micron aerosol in marine boundary layer (MBL) air masses from the remote Southern Ocean, Western Europe, the Iberian coast, the Mediterranean and the background Atlantic Ocean. The differences in these aerosol properties, combined with dimethylsulfide, sulfur dioxide and meteorological measurements provide a means to assess processes that affect the aerosol distribution. The background sub-micron aerosol measured over the Atlantic Ocean during ACE-2 was more abundant (number and volume) and appeared to be more aged than that measured over the Southern Ocean during ACE-1. Based on seawater DMS measurements and wind speed, the oceanic source of non-sea-salt sulfur and sea-salt to the background marine atmosphere during ACE-1 and ACE-2 was similar. However, the synoptic meteorological pattern was quite different during ACE-1 and ACE-2. The frequent frontal passages during ACE-1 resulted in the mixing of nucleation mode particles into the marine boundary layer from the free troposphere and relatively short aerosol residence times. In the more stable meteorological setting of ACE-2, a significant nucleation mode aerosol was observed in the MBL only for a half day period associated with a weak frontal system. As a result of the longer MBL aerosol residence times, the average background ACE-2 accumulation mode aerosol had a larger diameter and higher number concentration than during ACE-1. The sub-micron aerosol number size distributions in the air masses that passed over Western Europe, the Mediterranean, and coastal Portugal were distinctly different from each other and the background aerosol. The differences can be attributed to the age of the air mass and the degree of cloud processing.

* Corresponding author.
e-mail: bates@pmel.noaa.gov

1. Introduction

Atmospheric aerosol-size distributions impact the radiative and cloud nucleating properties of aerosols. A better understanding of the regional variations in these distributions and the processes controlling them is fundamental to improving aerosol process and climate models. In recent years, measurements and models have identified a number of key features in unperturbed marine boundary layer (MBL) size distributions and the processes that control them (Hoppel et al., 1986, 1990; Hegg et al., 1990, 1992; Covert et al., 1992; Raes and Van Dingenen, 1992; Sievering et al., 1992; Clarke, 1993; Gras, 1993; Ito, 1993; O'Dowd and Smith, 1993; Hoppel et al., 1994; Perry and Hobbs, 1994; Russell et al., 1994; Raes, 1995; Clarke et al., 1996; Covert et al., 1996a,b; Wiedensohler et al., 1996; Gong et al., 1997; Bates et al., 1998a; Brechtel et al., 1998; Clarke et al., 1998a,b; Kreidenweis et al., 1998; Weber et al., 1998). However, continentally influenced air masses substantially alter these background size distributions and thus affect the overall aerosol radiative and cloud nucleating properties. Measurements in a globally representative range of natural and anthropogenically perturbed environments are needed to assess the extent of this perturbation, the resulting changes in aerosol properties, and the atmospheric processes that determine the extent, timing, and magnitude of the perturbation.

The gas and aerosol measurements made aboard the RV *Discoverer* during ACE-1 (Bates et al., 1998b) provided a means to characterize aerosol properties and assess processes that affect the aerosol distribution in the lower MBL south of Tasmania (Bates et al., 1998a). In this paper we present similar measurements from ACE-2 (Raes et al., 2000) and compare background submicrometer aerosol-size distributions in the two regions and different continentally influenced air masses in the ACE-2 region. Additional complementary ACE-2 shipboard measurements, including aerosol chemical and optical properties (Quinn et al., 2000), hygroscopic properties (Swietlicki et al., 2000), and organic characterization (Novakov et al., 2000), are included in this special issue.

2. Methods

The aerosol and gas sampling methods were similar in ACE-1 and ACE-2. Aerosol particles were sampled at 18 m (ACE-1) or 10 m (ACE-2) above sea level (asl) through a heated mast (Bates et al., 1998b). The mast extended 6 m above the aerosol measurement container and was capped with a cone-shaped inlet nozzle that was rotated into the relative wind. Air was drawn through this 5 cm diameter inlet nozzle at $1\ m^3\ min^{-1}$ and down the 20-cm diameter mast. The lower 1.5 m of the mast were heated to dry the aerosol to a relative humidity (RH) of $55 \pm 5\%$. Fifteen 1.9 cm diameter electrically conductive polyethylene tubes extending into this heated zone were used to subsample the air stream for the various aerosol sizing/counting instruments and impactors at flows of $30\ l\ min^{-1}$. Comparisons of the total particle count ($D_p > 3$ nm) during intercomparisons with the NCAR C-130 and ACE-1 ground stations agreed to within 20% suggesting minimal loss of particles in the inlet system (Weber et al., 1999).

Total particle number was measured with condensation particle counters (CPC, TSI model 3010 and UCPC, TSI model 3025). The CPC and UCPC measure all particles larger than roughly 12 and 3 nm, respectively. The total particle counts from each instrument were recorded each minute. The number size distribution between 5 and 600 nm was measured every 10 min with two differential mobility particle sizers (DMPS, TSI model 3071 mobility analyzer plus CPC and Hauke mobility analyzer plus UCPC) at an RH of approximately 10% (ACE-1) or 45% (ACE-2). The data were filtered to eliminate periods of calibration and instrument malfunction and periods of ship contamination (based on relative wind and high CN counts). The filtered mobility distributions from the DMPSs were converted to number-size distributions using the inversion routine of Stratman and Wiedensohler (1997). The data were corrected for diffusional losses (Covert et al., 1997) and size dependent counting efficiencies (Wiedensohler et al., 1997) based on pre-ACE-1 and ACE-2 intercalibration exercises. The 10 min number distributions were averaged into 30 min periods centered on the hour and half-hour. An interactive routine was used to fit lognormal curves to the several modes of the number size distribution. Assuming (1) an external mixture of sea-salt and non-sea-salt sulfate and (2) the coarse mode(s) consisted of sea-salt and the accumulation and Aitken modes consisted of the non-

sea-salt sulfate, the number size distribution was shifted from 45% RH to dry (10% RH) using growth factors of 1.4 for sea-salt and 1.15 for non-sea-salt (nss) sulfate aerosol (Swietlicki et al., 2000). The integral of the number size distribution was $69 \pm 4.5\%$ of the total number concentration measured with the TSI 3025. The difference is most likely a result of losses in Aitken mode and smaller particles in the DMPS in excess of the typical losses in a model 3071 mobility analyzer.

Air samples for DMS analysis were collected through a Teflon line which ran approximately 60 m from the top of the aerosol sampling mast to the analytical system. One hundred ml min^{-1} of the 4 l min^{-1} flow were pulled through a KI solution at the analytical system to eliminate oxidant interferences. The air sample volume ranged from 0.5 to 1.5 l depending on the DMS concentration. Seawater samples were collected from the ship's seawater pumping system at a depth of approximately 5 m (bow inlet) during ACE-1 and 3 m (mid-ship inlet) during ACE-2. The seawater line ran to the analytical system where 5.1 ml of sample were valved into a Teflon gas stripper. The samples were purged with hydrogen at 80 ml min^{-1} for 5 min. Water vapor in either the air or purged seawater sample stream was removed by passing the flow through a $-25°C$ Teflon tube filled with silanized glass wool. DMS was then trapped in a $-25°C$ Teflon tube filled with Tenax. During the sample trapping period, 6.2 pmoles of methylethyl sulfide (MES) were valved into the hydrogen stream as an internal standard. At the end of the sampling/purge period the coolant was pushed away from the trap and the trap was electrically heated. DMS was desorbed onto a DB-1 mega-bore fused silica column where the sulfur compounds were separated isothermally at 50°C and quantified with a sulfur chemiluminesence detector. The system was calibrated using gravimetrically calibrated DMS and MES permeation tubes. The precision of the analysis, based on both replicate analyses of a single water sample and replicate analyses of a standard introduced at the inlet of the air sample line, was typically $\pm 8\%$. The detection limit was approximately 0.8 pmole. The performance of the system was monitored regularly by running blanks and standards through the entire system. Values reported here have been corrected for recovery losses. Losses within the system were $<10\%$. System blanks were below detection limit. Air samples are reported in units of parts-per-trillion by volume (ppt). The mixing ratios were calculated at standard temperature (25°C) and pressure (1013 hPa) such that 1 nmole/m^3 equals 24.5 ppt.

Sulfur dioxide (SO_2) was measured with a standard TECO SO_2 analyzer. Ambient air was drawn into the instrument through a 0.63 cm OD, 30 cm Telfon inlet-tube, a Teflon filter, a nafion drier, and finally 3 m of Teflon tubing at a flow rate 450 ml/min. The inlet tube was located 4 m above sea level at the front of the aerosol sampling container. The filter and drier were located in the aerosol sampling container and were heated to maintain the inlet air at 50% RH. The system was calibrated daily using gravimetrically calibrated SO_2 permeation tubes. The standard gas (3.8 or 1 ppb) and SO_2 free gas (generated by scrubbing ambient air with activated charcoal) were introduced to the system up-stream of the Teflon filter. The detection limit during ACE-2 was 0.1 parts-per-billion by volume (ppb). The mixing ratios were calculated at standard temperature (25°C) and pressure (1013 hPa) such that 1 nmole/m^3 equals 24.5 ppt.

The signal from the TECO SO_2 analyzer was recorded as 1 min averages. The data were filtered to eliminate periods of calibration and zero, periods when the wind was abaft the beam and

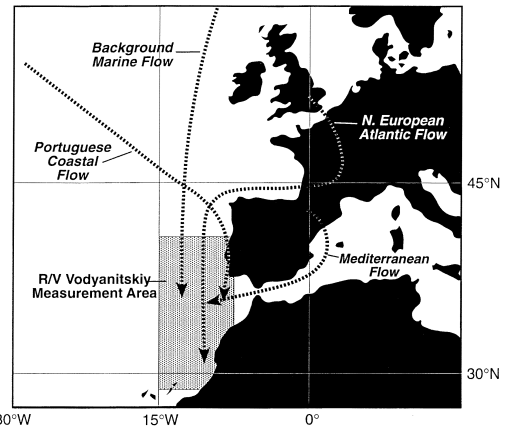

Fig. 1. ACE-2 study area showing the region sampled by the ship and approximate 5-day isentropic back trajectories for the air mass types discussed in the text. The background Atlantic trajectory (not shown) was similar to the Portuguese Coastal Flow trajectory but did not contact the coast.

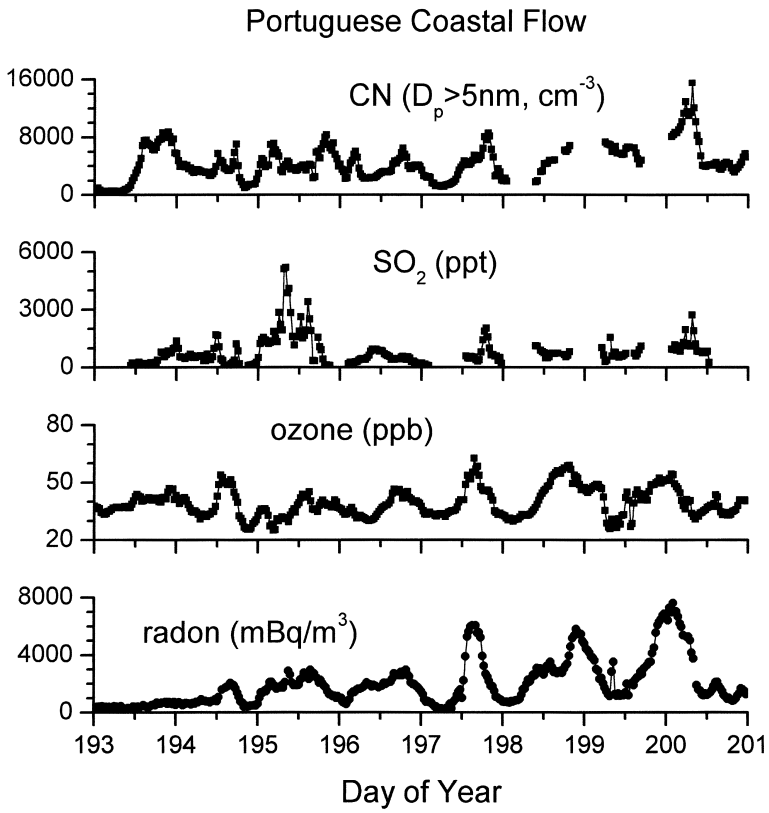

Fig. 2. Total aerosol number, radon and trace gas concentrations plotted as functions of day of year (DOY for 12 July to 20 July) during a period of Portuguese coastal flow showing the highly variable concentrations.

thus possibly subject to ship contamination, and during spikes of high SO_2 from passing ships (identified by spikes of high CN counts). The filtered 1 min data were averaged into 30-min periods centered on the hour and half-hour.

Aerosol chemical sampling was conducted with Berner-type multijet cascade impactors. Air was sampled only when the relative wind direction was forward of the beam, the relative wind speed was greater than 3 m s^{-1}, and the total particle count indicated the air was free of ship contamination. Further details of the sampling and ion chromatographic and gravimetric analysis are reported elsewhere (Quinn et al., 1998; Quinn et al., 2000). The 50% aerodynamic cutoff diameters of the impactors (Quinn et al., 1998) were converted to geometric diameters by dividing by the square root of the particle density. The densities were calculated using the analyzed chemical mass during the experiments and the chemical equilibrium model AeRho (Quinn and Coffman, 1998). The mass size distributions were dried to 10% RH using growth factors of 1.4 for sea-salt and 1.15 for non-sea-salt sulfate aerosol. Values reported in this paper as sub-micron refer to the first four impactor stages which translates to a 50% geometric dry cutoff diameter of 0.8 μm. The mixing ratios were calculated at standard temperature (25°C) and pressure (1013 hPa) such that 1 nmole/m^3 equals 24.5 ppt.

Additional measurements made aboard the ship included atmospheric temperature, pressure, and humidity, surface seawater temperature, salinity and nitrate concentrations, wind speed and direction, rainfall rates, solar radiation, atmospheric radon (Whittlestone and Zahorowski, 1998), and

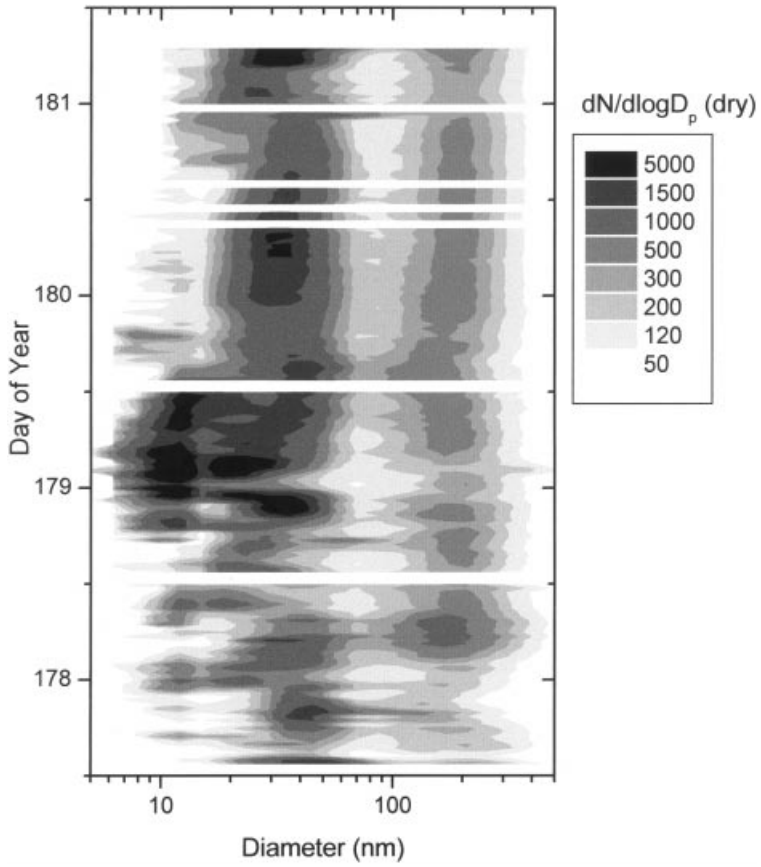

Fig. 3. ACE-2 sub-micron aerosol dry number size distribution (dN/d log D) during a period of background marine flow (26–30 June 1997). The legend values refer to the upper dN/d log D for that color shade.

vertical profiles of temperature, dewpoint temperature, and wind speed and direction from radiosondes. The back trajectories, calculated by the Royal Netherlands Meteorological Institute (KNMI), are based on ECMWF 3-D windfields with a resolution of $1^\circ \times 1^\circ$ (Scheele et al., 1996). All references to time are reported here in UTC. Dates are given as Day of Year (DOY) where noon on 1 February equals DOY 32.5.

3. Results and discussion

3.1. *Oceanographic settings and ocean–atmosphere DMS flux*

The intensive ACE-1 campaign (15 November to 14 December 1995) covered three distinct water masses in the region south and west of Tasmania, Australia. Seawater DMS concentrations and ocean–atmosphere fluxes were highest in the Subtropical Convergence Zone to the north and lowest in the Polar Water to the south (Bates et al., 1998a). ACE-2 (16 June–24 July 1997) was conducted in one water mass on the eastern edge of the North Atlantic gyre (Fig. 1). Sea surface temperature and salinity in the ACE-2 region varied linearly with latitude ranging from 23°C, 36.8 PSU in the south (29°N) to 18°C, 35.8 PSU in the north (41°N). Nitrate concentrations in these waters were less than 0.05 μM and chlorophyll concentrations were generally less than 0.07 μg/l. Surface seawater DMS concentrations during ACE-2 were relatively uniform during the first 3 weeks of the campaign averaging

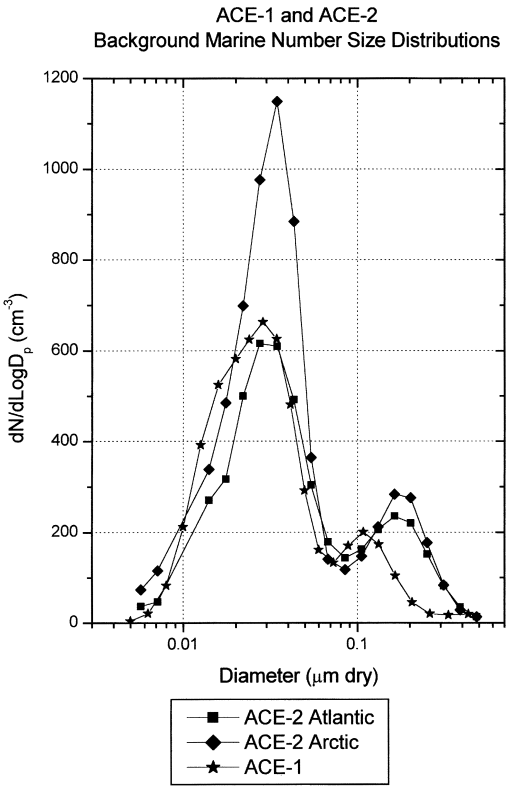

Fig. 4. Background MBL aerosol dry number size distributions for ACE-1 and ACE-2. The ACE-1 distribution, showing a large nucleation mode shoulder on the Aitken mode, was obtained from a log-normal fit to the average fitted data (Table 1). The ACE-2 data are an average of the size distributions during the time periods of Atlantic and Arctic flow.

1.3 ± 0.2 nM (data from distances greater than 40 km from the coast). During the final week, concentrations in the offshore region west of Portugal began to increase, reaching 2.7 nM by the end of the campaign. Using shipboard measured winds, surface water DMS concentrations and the wind speed transfer velocity relationship of Liss and Merlivat (1986), the calculated average ocean to atmosphere flux of DMS was 4.7 ± 5.0 μmol/m^2/d and 5.4 ± 3.2 μmol/m^2/d, in ACE-1 and ACE-2, respectively (Table 1). Although we cannot rule out regions of higher/lower DMS fluxes upwind of the study areas, the comparable fluxes within the study areas suggest a similar natural source of sulfur to the atmospheric aerosol in the two regions during the time of the experiments.

3.2. Meteorological settings

During the ACE-1 intensive campaign, the synoptic weather pattern was very active with 14 cold fronts passing through the area and 6 low-pressure systems distinctly cut off from the prevailing westerlies (Hainsworth et al., 1998). The air masses sampled at the ship were typical of background marine conditions in the midlatitudes with very low radon concentrations (<100 mBq m^{-3}) and a mean total ($D_p > 3$ nm) particle number concentration of 500 cm^{-3} (Bates et al., 1998a).

In sharp contrast to the active weather patterns during ACE-1, weather patterns in the ACE-2 study area were dominated by the Azores high producing winds from the northwest to northeast 90% of the time. In general, the atmosphere was thermally stable with boundary layer heights <1 km. Based on observations from the ship, the sky was $>50\%$ cloud covered 60% of the time. Frontal systems usually passed to the north of the ACE-2 area. The passage of these frontal systems and the thermal lows that occasionally developed over the European continent, affected the air mass trajectories reaching the ACE-2 region. The air masses sampled at the ship during ACE-2 can be classified into five groups (Fig. 1) based on calculated back trajectories (Verver et al., 2000). The ship encountered background Atlantic/Arctic marine air masses approximately 38% of the time, Mediterranean flow 6% of the time, Western European air flow 18% of the time and air flowing along the Portuguese coast 38% of the time. Airflow along the Portuguese coast resulted in strong gradients in gaseous and aerosol species (Fig. 2), making comparisons between platforms in this region difficult.

3.3. Comparison of the ACE-1 and ACE-2 background marine aerosol

The number size distributions of the background aerosol in the Southern Ocean (ACE-1) and Atlantic Ocean (ACE-2) MBL can be described by 4 distinct modes: a nucleation mode (referred to in Bates et al. (1998a) as the ultrafine mode) ($D_p \approx 5$–20 nm), an Aitken mode ($D_p \approx 20$–100 nm), an accumulation mode ($D_p \approx$

Table 1. *Background marine aerosol*

		ACE-1	ACE 2	
DMS, seawater				
(>40 km from coast)	mean, (nM)	1.7 ± 1.1	1.6 ± 0.5	
	median	1.3	1.4	
DMS, flux	mean (μmol/m^2/d)	4.7 ± 5.0	5.1 ± 2.9	
(>40 km from coast)	median	3.4	4.4	
DMS, atmosphere	mean (ppt)	110 ± 61	79 ± 45	
(background marine conditions)	median	96	68	
			Atlantic flow	Arctic flow
nucleation mode	N (cm^{-3})	190 ± 180	60 ± 70	120 ± 150
(dry)	D_{gn} (nm)	16 ± 0.55	14 ± 3.3	14 ± 3.4
	σ_g	1.45 ± 0.55	1.19 ± 0.16	1.22 ± 0.13
Aitken mode	N (cm^{-3})	210 ± 160	235 ± 125	420 ± 220
(dry)	D_{gn} (nm)	33 ± 6.8	37 ± 9.3	36 ± 6.0
	σ_g	1.40 ± 0.16	1.43 ± 0.13	1.38 ± 0.14
accumulation mode	N (cm^{-3})	74 ± 35	110 ± 70	110 ± 36
(dry)	D_{gn} (nm)	110 ± 25	170 ± 24	170 ± 17
	σ_g	1.41 ± 0.09	1.44 ± 0.06	1.42 ± 0.05
sub-micron volume[a)]	μm^3 cm^{-3}	0.11 ± 0.05	0.67 ± 0.42	0.81 ± 0.18
(Aitken and accumulation modes)		0.095	0.53	0.51
sub-micron nss sulfate + ammonium	μg^3 m^{-3}	0.19 ± 0.06	0.74 ± 0.20	0.67 ± 0.12
(<0.8 μm dry geometric diameter)				

Means are given with ± 1 SD.

[a)] The top value given for sub-micron volume was calculated from the number of particles in each bin of the DMPS. The bottom value was calculated from the modal parameters given in this table.

100–500 nm), and a coarse mode ($D_p > 500$ nm). We will limit our discussion in this paper to the dominant (by number) 3 smaller modes (Table 1).

During ACE-1 the nucleation mode was a major feature in the number size distribution 50% of the time (Fig. 4). The observed periods of high nucleation mode particle concentrations coincided with the passage of cold fronts and regions of high convective activity associated with cumulus clouds (Bates et al., 1998a). In the more stable meteorological setting of ACE-2, a nucleation mode was observed at the ship only for a one half-day period (DOY 178.9–179.5, 27–28 June, Fig. 3) in a region of broken convective clouds behind a weak frontal system. Boundary layer heights before the passage of this front were <500 m but rose to 1500–2000 m during and after the frontal passage. Although we have no measurements in this region at this time to confirm the presence or absence of nucleation mode particles in the free troposphere (FT), the presence of nucleation mode particles in the MBL during this period of convective mixing is consistent with our observations from ACE-1 and suggests a FT source for these particles.

Other measurements from ACE-2 are consistent with our shipboard observations. Measurements aboard the CIRPAS *Pelican* found no evidence of nucleation mode particles during ACE-2 in the MBL (Collins et al., 2000). Conversely, measurements in the upper FT aboard a Cessna Citation aircraft found evidence for new particle formation and growth (M. deReus, personnel communication). The shipboard and aircraft data from ACE-1 and ACE-2 are consistent with the theory that nucleation mode particles are rarely formed over the ocean in background MBL air masses (Hegg et al., 1990; Raes and Van Dingenen, 1992; Clarke, 1993; Hegg et al., 1993; Hoppel et al., 1994; Raes, 1995; Covert et al., 1996a,b; Clarke et al., 1998a,b). Concentrations of precursor gases are generally too small to promote new particle production in this region of high sea-salt particle surface area

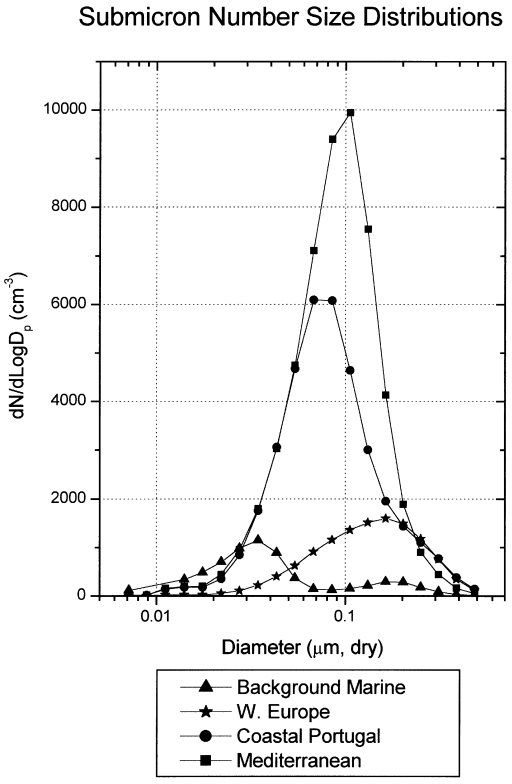

Fig. 5. Average aerosol dry number size distributions during periods when the MBL was influenced by flow over the continent. The average size distribution during periods of background Arctic flow (Fig. 4) is shown for comparison.

(Hegg et al, 1992; Raes et al., 1995). Sea-salt was always a major component of the aerosol in ACE-1 and ACE-2 in both background marine and continentally modified air-masses (Neususs et al., 2000; Putaud et al., 2000; Quinn et al., 1998, 2000). Average aerosol dry surface areas ($5\ \text{nm} < D_p < 3500\ \text{nm}$) during the periods of background marine air masses of ACE-1 (18 m asl) and ACE-2 (10 m asl) were 40 ± 22 and $31 \pm 11\ \mu\text{m}^2\ \text{cm}^{-3}$, respectively.

The ubiquitous features in marine aerosol number size distributions are the well-defined Aitken and accumulation modes that result from cloud processing (Hoppel et al., 1986, 1990). These modes were clearly evident in both ACE-1 and ACE-2 (Fig. 4) although the mean diameters and number concentrations differed. The number concentrations of the Aitken and accumulation modes were higher during ACE-2 than ACE-1 (Table 1, Fig. 4). In addition, the mean diameter of the accumulation mode was higher in ACE-2 than ACE-1. The distributions are consistent with our current understanding of the sources and sinks of these particles and the meteorological conditions during the two experiments. Aitken mode particles in the remote MBL originate from the condensational growth and coagulation of nucleation mode particles (Hoppel et al., 1990) and more commonly from entrainment from aloft (Clarke et al., 1996, 1997). The large-scale subsidence that accompanied the background marine ACE-2 air masses (Verver et al., 2000; Johnson et al., 2000a) are the most likely source of these MBL Aitken mode particles. Note the average concentration of Aitken mode particles observed during Arctic marine flow ($420\ \text{cm}^{-3}$) was appreciably higher than during mid-Atlantic marine flow ($235\ \text{cm}^{-3}$) which is consistent with a stronger subsidence during the periods of Arctic flow (Verver et al., 2000). Aircraft measurements during the first ACE-2 Lagrangian experiment, which was conducted in a background marine air mass (Johnson et al., 2000b), indicated periods of elevated concentrations of aerosols with diameters < 100 nm above the MBL. An alternate source for these particles is from long range transport from continental sources in either North America or Western Europe. However, calculated backtrajectories (Verver et al., 2000; Johnson et al., 2000a) and shipboard atmospheric ^{222}Rn measurements suggest the air masses identified here as background marine had not been in contact with the continent for < 5 days.

The major sink for Aitken mode particles is coagulation with other Aitken mode particles and cloud processing which leads to growth by liquid phase conversion of trace gases to nonvolatile solute compounds (Hoppel and Frick, 1990; Hoppel et al., 1996). Based on the water supersaturation level in the cloud, some particles will eventually grow sufficiently large to activate and form cloud droplets. When the cloud dissipates, the interstitial (unactivated) particles and residual (from evaporated cloud droplets) particles remain. This process is thought to differentiate the Aitken and accumulation modes with the MBL cloud supersaturation and aerosol chemistry defining the diameter of the intermode minimum (Hoppel et al., 1986; 1994). The larger diameter and higher average number concentration of the accumula-

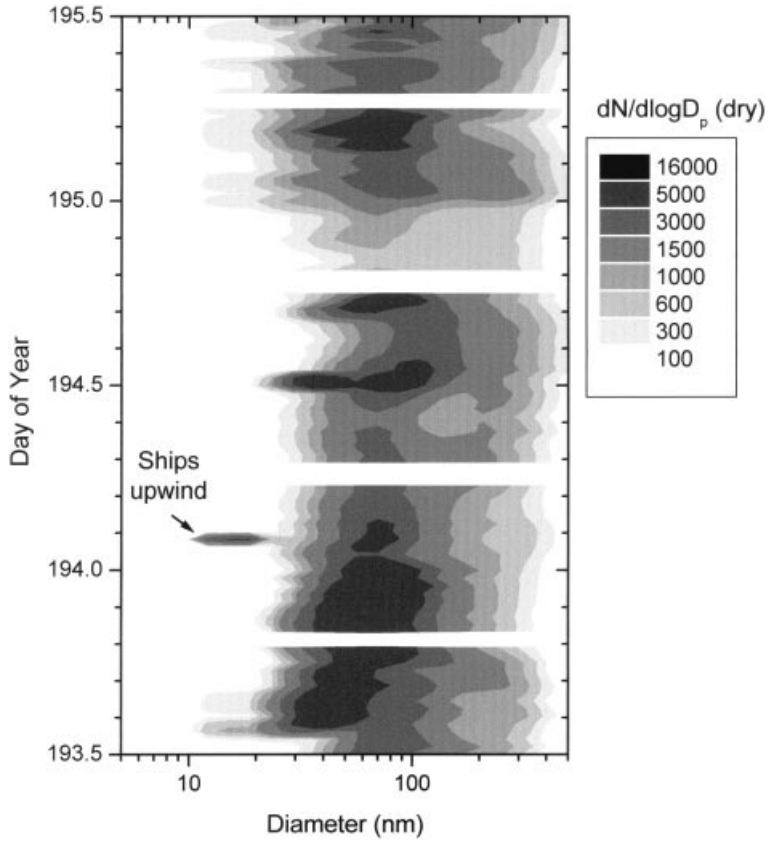

Fig. 6. Aerosol dry number size distribution (dN/d log D) during a period of Portuguese coastal flow (12–14 July 1997). The legend values refer to the upper dN/d log D for that color shade.

tion mode during ACE-2 (Fig. 4, Table 1) are consistent with enhanced condensational growth and liquid phase oxidation of soluble trace gases during cloud processing (Hoppel et al., 1996) and are similar to previous measurements in the Azores high (Hoppel et al., 1990; Jensen et al., 1996; Clarke et al., 1997). The sulfur gases available for condensational growth appear to be of similar magnitude in ACE-1 and ACE-2. Although SO_2 concentrations measured at the ship during the background conditions of ACE-2 were below the instrumental detection limit (100 ppt), MBL SO_2 measurements taken at Punta del Hidalgo on Tenerife (J. P. Putaud, personnel communication) and aboard the Meteorological Research Flights's C-130 Aircraft (Johnson et al., 2000b) during background marine conditions show average concentrations of approximately 20 ppt (range from a few ppt to 100 ppt). This compares with an average background SO_2 concentration during ACE-1 of 12 ± 7.6 ppt (DeBruyn et al., 1998). Similarly, the natural source of sulfur (DMS) from the ocean to the atmosphere appears to be similar in magnitude in ACE-1 and ACE-2 (Table 1), although we cannot rule out an enhanced DMS source upwind of the ACE-2 area in the higher latitude regions often dominated by coccolithophore blooms (Malin et al., 1993). Although the concentration of condensable species may not have been significantly higher in ACE-2 than ACE-1, enhanced condensational growth also can result from longer MBL residence times. The frequent frontal passages during ACE-1 resulted in relatively short MBL aerosol residence times

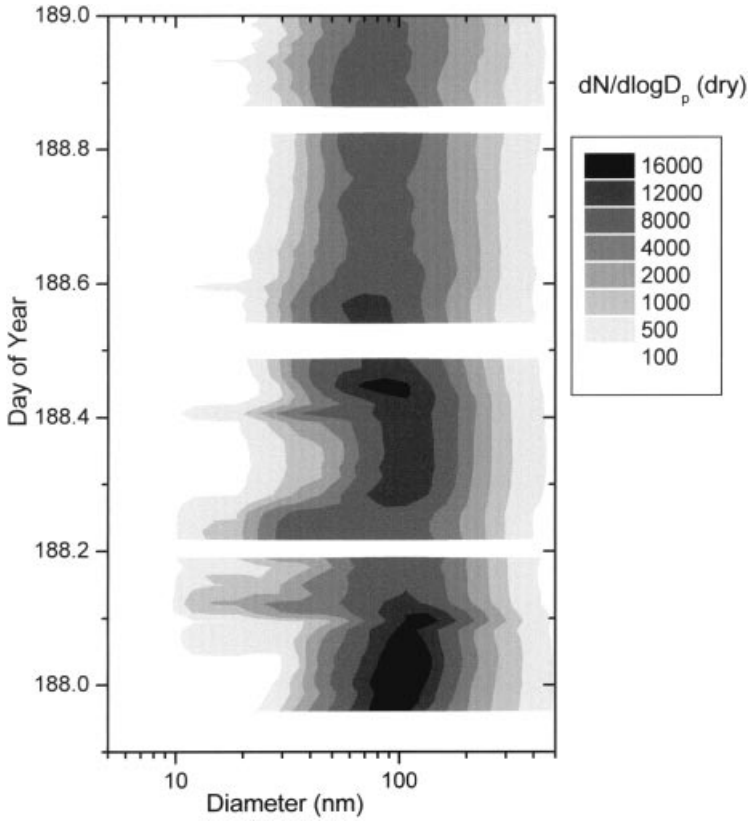

Fig. 7. Aerosol dry number size distribution (dN/d log D) during period of Mediterranean flow (6–8 July 1997). The legend values refer to the upper dN/d log D for that color shade.

due to convective mixing and precipitation. Conversely, the more stable meteorological conditions during ACE-2 resulted in longer MBL aerosol residence times (several days based on back trajectory analysis). Similar results have been reported for the tropical regions of the Pacific (Covert et al., 1996a) where long MBL air mass residence times (>5 days) lead to enhanced accumulation mode number and larger modal diameters.

An additional source of accumulation mode particles is direct production from the sea surface (O'Dowd and Smith, 1993). Sea-salt particles dominated the accumulation mode number and mass during ACE-1 (Murphy et al., 1998; Quinn et al., 1998). Although the sea-salt sub-micron mass was similar in ACE-1 and ACE-2 (Quinn et al., 2000), it did not dominate the sub-micron mass in the background MBL during ACE-2 (Putaud et al., 2000; Quinn et al., 2000) due to the presence of higher concentrations of other species. The importance of sea-salt particles to accumulation mode number was not directly quantified during ACE-2. However, a time-scale analysis of background MBL aerosol evolution during the first Lagrangian experiment suggests that the enhancement of accumulation mode aerosol during the course of the Lagrangian, as wind speed increased, could be ascribed to enhanced sea-salt aerosol flux (Hoell et al., 2000). Although the direct measurements of ACE-1 and the time-scale analysis of ACE-2 show that sea-salt particles can be an important component of the accumulation mode number concentration, there was no correlation between wind speed and accumulation mode number concentration during ACE-1 or ACE-2.

Table 2. *Continentally modified aerosol*

		Coastal Portugal	Mediterranean	W. Europe
SO_2	ppt	840 ± 760	610 ± 410	160 ± 90
ozone	ppb	39 ± 7.6	54 ± 10	45 ± 5.3
DMS, atmosphere	ppt	54 ± 44	40 ± 26	51 ± 25
average cloud cover	%	62	6	56
Aitken mode	N (cm^{-3})	2800 ± 1900	4600 ± 1300	650 ± 310
(dry)	D_{gn} (nm)	76 ± 15	105 ± 15	93 ± 21
	σ_g	1.52 ± 0.13	1.51 ± 0.06	1.60 ± 0.11
accumulation mode	N (cm^{-3})	350 ± 160		420 ± 190
(dry)	D_{gn} (nm)	230 ± 41		220 ± 39
	σ_g	1.36 ± 0.14		1.37 ± 0.08
sub-micron volume[a)]	$\mu m^3\ cm^{-3}$	5.9 ± 2.0	5.5 ± 1.8	5.0 ± 1.7
(Aitken and accumulation modes)		4.8	4.8	4.4
sub-micron nss sulfate + ammonium (<0.8 μm dry geometric diameter)	$\mu g^3\ m^{-3}$	7.9 ± 2.4	6.6 ± 1.8	7.7 ± 1.9

Means are given with ± 1 standard deviation.
[a)] The top value given for sub-micron volume was calculated from the number of particles in each bin of the DMPS. The bottom value was calculated from the modal parameters given in this table.

Even though an increase (decrease) in wind speed increases (decrease) the flux of sea-salt particles to the atmosphere, a change in wind speed does not necessarily change the MBL number or mass concentration of sea-salt particles since the concentration is also a function of the MBL height and sink processes.

3.4. *Comparison of ACE-2 modified continental aerosols*

The modified continental aerosols reaching the ship during ACE-2 were divided into three regions of origin. Although the sub-micron aerosol did not show the clear bimodal structure ubiquitous in the background marine distributions, the number size distribution was usually best-fit by the sum of two lognormal modes, an Aitken and an accumulation mode (Table 2, Fig. 5). A significant nucleation mode was not present in any of the modified continental air masses and appeared only when ships passed upwind (Fig. 6). The sub-micron aerosol mass in the continentally modified air masses during ACE-2 was dominated by the nss sulfate aerosol (nss sulfate + ammonium) (Quinn et al., 2000) with average values ranging from 6.6 to 7.9 $\mu g\ m^{-3}$ (1.7 to 2.0 ppb) (Table 2). Total Aitken and accumulation mode aerosol volume in the air masses from the three continental regions covered a limited range from 5.0 to 5.9 $\mu m^3\ cm^{-3}$ despite the markedly different number size distributions (Table 2).

The air masses that advected along the coast of Portugal were subjected to local point sources (Verver et al., 2000) and were thus the least aged. The measured concentrations of gases and particles were highly variable (Figs. 2, 6) depending on the trajectory and the distance between the ship and the coast. Being close to the source, SO_2 concentrations were higher than in the other air masses (Table 2). The dominant mode in the number size distribution was centered at 76 nm while the secondary accumulation mode was centered at 230 nm (Fig. 5). The modal parameters of these size distributions are very similar to those measured off the coast of Portugal by Hoppel et al. (1990).

The aerosol coming from the Mediterranean had a dominant mode in the number size distribution centered at 105 nm (Figs. 5, 7). SO_2 and O_3 concentrations in this air mass were high (610 ppt and 54 ppb, respectively). The total aerosol number concentration was the highest measured during ACE-2. The size distribution was unique in that there was no identifiable accumulation mode. The average cloud cover during this period

was only 6% as opposed to approximately 60% during the other time periods (Table 2) which would suggest a near absence of cloud processing. It is also interesting to note that this aerosol contained the lowest fraction of nss sulfate + ammonium and the highest concentrations of organic and black carbon (Quinn et al., 2000).

The aerosol that originated over Western Europe and advected 1500 km over the ocean (Fig. 1) was well aged with primary and secondary modes in the number size distribution centered at 93 and 220 nm (Figs. 5, 8). SO_2 concentrations in this air mass were generally below the detection limit of 100 ppt.

We attribute the differences in the size distributions in these three air masses to the time spent in the MBL and the degree of cloud processing. The least aged aerosol had the smallest diameter particles and was in an air mass with the highest concentration of SO_2 (coastal Portugal). Condensational growth and coagulation with time increase the Aitken modal diameter while cloud processing creates an accumulation mode. This evolution was clearly seen in the Lagrangian experiment that followed this "coastal" air mass (Johnson et al., 2000b; Osborne et al., 2000). On the other hand, little evolution was seen in the Lagrangian experiment that followed the more "aged" Western European aerosol (Johnson et al., 2000b; Wood et al., 2000) which suggests that the "processing" had largely taken place by the time the air mass reached the ACE-2 study area.

Aerosols in the continentally modified air masses completely dwarfed the background MBL aerosol (Fig. 5). The total sub-micron volume of the continentally modified air masses was an order

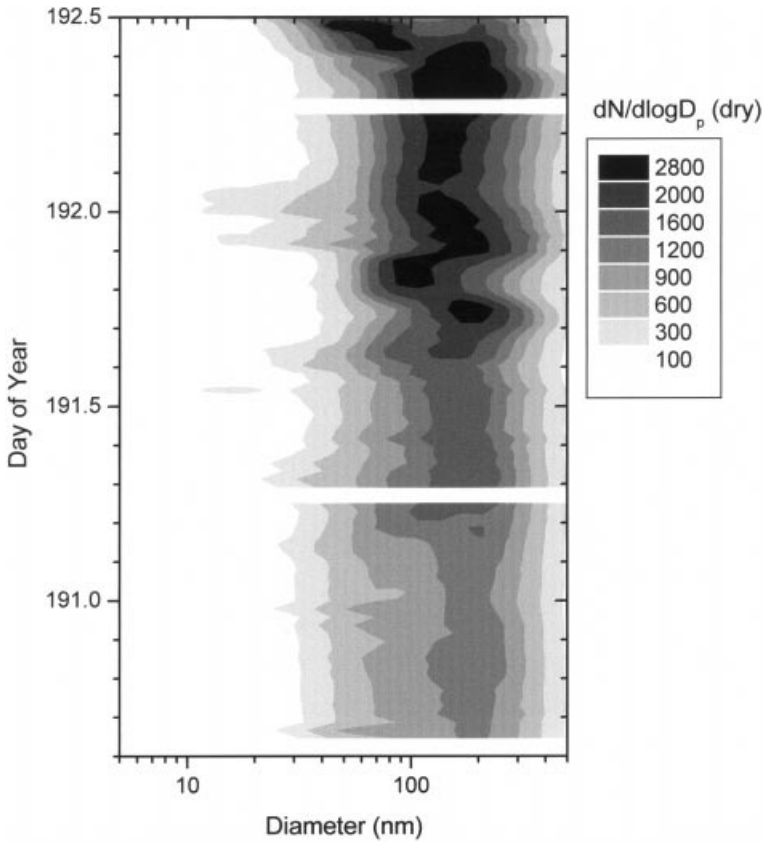

Fig. 8. Aerosol dry number size distribution ($dN/d \log D$) during period of Northern European flow (9–11 July 1997). The legend values refer to the upper $dN/d \log D$ for that color shade.

of magnitude higher than the background marine atmosphere (Tables 1 and 2).

4. Conclusions

Measurements of aerosol number size distributions during ACE-1 and 2 were used to define the physical aerosol properties in the different air masses of the two regions. The background submicron aerosol measured over the Atlantic Ocean during ACE-2 was more abundant (number and volume) and appeared to be more aged than that measured over the Southern Ocean during ACE-1. Based on seawater DMS concentrations and wind speed, the marine source of DMS and sea-salt to the atmospheric aerosol was similar within the two regions. The differences in the average size distributions were most likely a result of the regional meteorology. ACE-1 occurred in a region of frequent frontal passages while ACE-2 occurred in a region dominated by a subtropical anticyclone. The "fair-weather" conditions during ACE-2 favored a longer MBL aerosol residence time.

The sub-micron aerosol number size distributions in the air masses that passed over Western Europe, the Mediterranean, and coastal Portugal were distinctly different. The modal characteristics suggest that the Western European aerosol was the most aged and the coastal Portugal aerosol was the least aged. Although the number size distributions of the different continentally influenced air masses were different, the total aerosol volumes were surprisingly consistent.

5. Acknowledgements

We thank Frank Stratmann, Sylvia Henning and the Institute of Tropospheric Research, Leipzig Germany, for the DMPS data inversions, Rita Van Dingenen and Frank Raes for their reviews of this manuscript and the officers and crew of the Institute of Biology of Southern Seas (Sebastopol, Ukrania) Research Vessel *Professor Vodyanitiskiy*. This research was funded by the Aerosol Project of the NOAA Climate and Global Change Program and the NOAA Office of Oceanic and Atmospheric Research. Financial support for ship time was provided by the European Commission DG XII (Environment and Climate) and the NOAA Office of Oceanic and Atmospheric Research. This is a contribution to the International Global Atmospheric Chemistry (IGAC) Core Project of the International Geosphere-Biosphere Programme (IGBP) and is part of the IGAC Aerosol Characterization Experiments (ACE). This is NOAA/PMEL contribution 2046 and JISAO contribution 651.

REFERENCES

Bates, T. S., Huebert, B. J., Gras, J. L., Griffiths, B. and Durkee, P. A. 1998b. The International Global Atmospheric Chemistry (IGAC) Project's First Aerosol Characterization Experiment (ACE-1): overview. *J. Geophys. Res.* **103**, 16,297–16,318.

Bates, T. S., Kapustin, V. N., Quinn, P. K., Covert, D. S., Coffman, D. J., Mari, C., Durkee, P. A., DeBruyn, W. and Saltzman, E. 1998a. Processes controlling the distribution of aerosol particles in the lower marine boundary layer during the First Aerosol Characterization Experiment (ACE-1). *J. Geophys. Res.* **103**, 16,369–16,384.

Brechtel, F., Kreidenweis, S. and Swan, H. 1998. Air mass characteristics, aerosol particle number concentrations and number size distributions at Macquarie Island during ACE-1. *J. Geophys. Res.* **103**, 16,351–16,367.

Clarke, A. D. 1993. Atmospheric nuclei in the Pacific midtroposphere: their nature, concentrations and evolution, *J. Geophys. Res.* **98**, 20,633–20,647.

Clarke, A. D., Li, Z. and Litchy, M. 1996. Aerosol dynamics in the equatorial Pacific marine boundary layer: microphysics, diurnal cycles and entrainment, *Geophys. Res. Lett.* **23**, 733–736.

Clarke, A. D., Uehara, T. and Porter, J. N. 1997. Atmospheric nuclei and related aerosol fields over the Atlantic: clean subsiding air and continental pollution during ASTEX. *J. Geophys. Res.* **102**, 25,281–25,292.

Clarke, A. D., Davis, D., Kapustin, V. N., Eisele, F., Chen, G., Paluch, I., Lenschow, D., Bandy, A. R., Thornton, D., Moore, K., Mauldin, L., Tanner, D., Litchy, M., Carroll, M. A., Collins, J. and Albercook, G. 1998a. Particle nucleation in the tropical boundary layer and its coupling to marine sulfur sources. *Science* **282**, 89–92.

Clarke, A. D., Varner, J. L., Eisele, F., Mauldin, R. L., Tanner, D. and Litchy, M. 1998b. Particle production in the remote marine atmosphere: cloud outflow and subsidence during ACE-1. *J. Geophys. Res.* **103**, 16,397–16,409.

Collins, D. R., Jonsson, H. H., Seinfeld, J. H., Flagan, R. C., Gasso, S., Hegg, D. A., Russell, P. B., Schmid, B.,

Livingston, J. M., Ostrom, E., Noone, K. J., Russell, L. M. and Putaud, J. P. 2000. In-situ aeorsol size distributions and clear column radiative closure during ACE-2. *Tellus* **52B**, 498–525.

Covert, D. S., Wiedensohler, A., Aalto, P., Heintzenberg, J., McMurry, P. H. and Leck, C. 1996b. Aerosol number size distributions from 3 to 500 nm diameter in the Arctic marine boundary layer during summer and autumn. *Tellus* **48**, 197–212.

Covert, D. S., Kapustin, V. N., Quinn, P. K. and Bates, T. S. 1992. New particle formation in the marine boundary layer. *J. Geophys. Res.* **97**, 20,581–20,590.

Covert, D. S., Kapustin, V. N., Bates, T. S. and Quinn, P. K. 1996a. Physical properties of marine boundary layer aerosol particles of the mid-Pacific in relation to sources and meteorological transport. *J. Geophys. Res.* **101**, 6919–6930.

Covert, D., Wiedensohler, A. and Russell, L. M. 1997. Particle charging and transmission efficiencies of aerosol charge neutralizers. *Aerosol Sci. and Technol.* **27**, 206–214.

De Bruyn, W. J., Bates, T. S., Cainey, J. and Saltzman, E. S. 1998. Shipboard measurements of DMS and SO_2 Southwest of Tasmania during ACE-1. *J. Geophys. Res.* **103**, 16,703–16,712.

Gong, S. L., Barrie, L. A. and Blanchet, J.-P. 1997. Modeling sea-salt aerosols in the atmosphere, 1, model development. *J. Geophys. Res.* **102**, 3805–3818.

Gras, J. L. 1993. Condensation nucleus size distribution at Mawson, Antarctica: microphysics and chemistry. *Atmos. Environ.* **27A**, 1427–1434.

Hainsworth, A., Dick, A. L. and Gras, J. L. 1998. Climatic context of ACE-1: a meteorological and chemical overview. *J. Geophys. Res.* **103**, 16,319–16,340.

Hegg, D. A., Radke, L. F. and Hobbs, P. V. 1990. Particle production associated with marine clouds. *J. Geophys. Res.* **95**, 13,917–13,926.

Hegg, D. A., Covert, D. S. and Kapustin, V. N. 1992. Modeling a case of particle nucleation in the marine boundary layer. *J. Geophys. Res.* **97**, 9851–9857.

Hegg, D. A., Ferek, R. J. and Hobbs, P. V. 1993. Aerosol size distributions in the cloudy atmospheric boundary layer of the North Atlantic Ocean. *J. Geophys. Res.* **98**, 8841–8846.

Hoell, C., O'Dowd, C., Johnson, D. W., Osborne, S. R. and Wood, R. 2000. A time-scale analysis of aerosol evolution in polluted and clean Lagrangian case studies. *Tellus* **52B**, 423–438.

Hoppel, W. A., Frick, G. M. and Larson, R. E. 1986. Effect of nonprecipitating clouds on the aerosol size distribution in the marine boundary layer. *Geophys. Res. Lett.* **13**, 125–128.

Hoppel, W. A. and Frick, G. M. 1990. Submicron aerosol size distributions measured over the tropical and south Pacific. *Atmos. Environ.* **24**, 645–659.

Hoppel, W. A., Fitzgerald, J. W., Frick, G. M. and Larson, R. E. 1990. Aerosol size distributions and optical properties found in the marine boundary layer over the Atlantic Ocean. *J. Geophys. Res.* **95**, 3659–3686.

Hoppel, W. A., Frick, G. M., Fitzgerald, J. W. and Larson, R. E. 1994. Marine boundary layer measurements of new particle formation and the effects nonprecipitating clouds have on aerosol size distributions. *J. Geophys. Res.* **99**, 14,443–14,459.

Hoppel, W. A., Frick, G. M. and Fitzgerald, J. W. 1996. Deducing droplet concentration and supersaturation in marine boundary layer clouds from surface aerosol measurements. *J. Geophys. Res.* **101**, 26,553–26,565.

Ito, T. 1993. Size distribution of Antarctic submicron aerosols. *Tellus* **45B**, 145–149.

Jensen, T. L., Kreidenweis, S. M., Kim, Y., Sievering, H. and Pszenny, A. 1996. Aerosol distributions in the North Atlantic marine boundary layer during Atlantic Stratocumulus transition experiment/marine aerosol and gas exchange. *J. Geophys. Res.* **101**, 4455–4467.

Johnson, D. W., Osborne, S., Wood, R., Suhre, K., Johnson, R., Businger, S., Quinn, P. K., Wiedensohler, A., Durkee, P. A., Russell, L. M., Andreae, M. O., O'Dowd, C., Noone, K., Bandy, B., Rudolph, J. and Rapsomanikis, S. 2000. An overview of the Lagrangian experiments undertaken during the North Atlantic Regional Aerosol Characterization Experiment (ACE-2). *Tellus* **52B**, 290–320.

Johnson, D. W., Osborne, S., Wood, R., Suhre, K., Quinn, P. K., Bates, T. S., Andreae, M. O., Noone, K., Glantz, P., Bandy, B., Rudolph, J. and O'Dowd, C. 2000. Observations of the evolution of the aerosol, cloud and boundary layer characteristics during the first ACE-2 Lagrangian Experiment. *Tellus* **52B**, 348–374.

Kreidenweis, S. M., McInnes, L. M. and Brechtel, F. J. 1998. Observations of aerosol volatility and elemental composition at Macquarie Island during ACE-1. *J. Geophys. Res.* **103**, 16,511–16,524.

Liss, P. S. and Merlivat, L. 1986. Air–sea gas exchange rates: introduction and synthesis. In: *The role of air–sea exchange in geochemical cycling* (ed. Buat-Menard, P), pp. 113–127. D. Reidel, Norwess, Mass.

Malin, G., Turner, S., Liss, P. and Holligan, P. 1993. Dimethylsulfide and dimethylsulphoniopropionate in the Northeast Atlantic during the summer coccolithophore bloom. *Deep-Sea Res.* **40**, 1487–1508.

Murphy, D. M., Anderson, J. R., Quinn, P. K., McInnes, L. M., Brechtel, F. J., Kreidenweis, S. M., Middlebrook, A. M., Posfai, M., Thomson, D. S and Buseck, P. R. 1998. Influence of sea-salt on aerosol radative properties in the Southern Ocean marine boundary layer. *Nature* **392**, 62–65.

Neusüß, C., Weise, D., Birmili, W., Wex, H., Wiedensohler, A. and Covert, D. 2000. Size segregated chemical, gravimetric and number distribution derived mass closure of the aerosol in Sagres, Portugal during ACE-2. *Tellus* **52B**, 169–183.

Novakov, T., Bates, T. S. and Quinn, P. K. 2000. Shipboard measurements of the concentration and

properties of carbon aerosols during ACE-2. *Tellus* **52B**, 228–237.

O'Dowd, C. D. and Smith, M. H. 1993. Physico-chemical properties of aerosol over the northeast Atlantic: evidence for wind speed related sub-micron sea-salt aerosol production. *J. Geophys. Res.* **98**, 1137–1149.

Osborne, S. R., Johnson, D. W., Wood, R., Bandy, B. J., Andreae, M. O., O'Dowd, C., Glantz, P., Noone, K., Rudolf, J., Bates, T. S. and Quinn, P. K. 2000. Observations of the evolution of the aerosol, cloud and boundary layer dynamic and thermodynamic characteristics during the second Lagrangian experiment of ACE-2. *Tellus* **52B**, 375–400.

Perry, K. D. and Hobbs, P. V. 1994. Further evidence for particle nucleation in clear air adjacent to marine cumulus clouds. *J. Geophys. Res.* **99**, 22,803–22,818.

Putaud, J. P., Van Dingenen, R., Mangoni, M., Virkkula, A., Raes, F., Maring, H., Prospero, J. M., Swietlicki, E., Berg, O., Hillamo, R. and Mäkelä, T. 2000. Chemical mass closure and origin assessment of the submicron aerosol in the marine boundary layer and the free troposphere at Tenerife during ACE-2. *Tellus* **52B**, 141–168.

Quinn, P. K. and Coffman, D. J. 1998. Local closure during ACE-1: aerosol mass concentration and scattering and backscattering coefficients. *J. Geophys. Res.* **103**, 16,575–16,596.

Quinn, P. K., Coffman, D. J., Kapustin, V. N., Bates, T. S. and Covert, D. S. 1998. Aerosol optical properties in the MBL during ACE-1 and the underlying chemical and physical aerosol properties. *J. Geophys. Res.* **103,**16,547–16,564.

Quinn, P. K., Bates, T. S., Coffman, D. J., Miller, T. L., Johnson, J. E., Covert, D. S. and Novakov, T. 2000. A comparision of aerosol chemical and optical properties from the first and second Aerosol Characterization Experiments. *Tellus* **52B**, 239–257.

Raes, F. 1995. Entrainment of free-tropospheric aerosol as a regulating mechanism for cloud condensation nuclei in the remote marine boundary layer. *J. Geophys. Res.* **100**, 2893–2903.

Raes, F. and Van Dingenen, R. 1992. Simulations of condensation nuclei and cloud condensation nuclei from biogenic SO_2 in the remote marine boundary layer. *J. Geophys. Res.* **97**, 12,901–12,912.

Raes, F. Bates, T. S., Van Liedekerke, M. and McGovern, F. M. 2000. The Second Aerosol Characterization Experiment (ACE-2): general overview and main results. *Tellus* **52B**, 111–125.

Russell, L. M., Pandis, S. N. and Seinfeld, J. H. 1994. Aerosol production and growth in the marine boundary layer. *J. Geophys. Res.* **99**, 20,989–21,003.

Scheele, M. P., Siegmund, P. C. and van Velthoven, P. F. J. 1996. Sensitivity of trajectories to data resolution and its dependence on the starting point: in or outside a tropopause fold. *Meteor. Appl.* **3**, 267–273.

Sievering, H., Boatman, J., Gorman, E., Kim, Y., Anderson, L., Ennis, G., Luria, M., and Pandis, S. 1992. Removal of sulphur from the marine boundary layer by ozone oxidation in sea-salt aerosol. *Nature* **360**, 571–573.

Stratman, F. and Wiedensohler, A. 1997. A new data inversion algorithm for DMPS measurements. *J. Aerosol Sci.* **27**, S1, 339–340.

Swietlicki, E., Zhou, J., Berg, O. H., Hameri, K., Vakeva, M., Makela, J., Covert, D. S., Dusek, U., Busch, B., Wiedensohler, A. and Stratmann, F. 2000. Hygroscopic properties of aerosol particles in the eastern Northern Atlantic during ACE-2. *Tellus* **52B**, 201–227.

Verver, G., Raes, F., Vogelezang, D. and Johnson, D. 2000. The Second Aerosol Characterization Experiment (ACE-2): meteorological and chemical context. *Tellus* **52B**, 126–140.

Weber, R. J., McMurry, P. H., Bates, T. S., Clarke, A. D., Covert, D. S., Brechtel, F. J. and Kok, G. L. 1999. Intercomparison of airborne and surface-based measurements of condensation nuclei in the remote troposphere during ACE-1. *J. Geophys. Res.*, in press.

Weber, R. J., McMurry, P. H., Mauldin, L., Tanner, D. J., Eisele, F. L., Brechtel, F. J., Kreidenweis, S. M., Kok, G. L., Schillawski, R. D. and Baumgardner, D. 1998. A study of new particle formation and growth involving biogenic trace gas species measured during ACE-1. *J. Geophys. Res.* **103**, 16,385–16,396.

Whittlestone, S. and Zahorowski, W. 1998. Baseline radon detectors for ship-board use: development and deployment in ACE-1. *J. Geophys. Res.* **103**, 16,743–16,751.

Wiedensohler, A., Covert, D. S., Swietlicki, E., Aalto, P., Heintzenberg, J. and Leck, C. 1996. Occurrence of an ultrafine particle mode less than 20 nm in diameter in the marine boundary layer during Arctic summer and autumn. *Tellus* **48**, 213–222.

Wiedensohler, A., Orsini, D., Covert, D. S., Coffmann, D., Cantrell, W., Havlicek, M., Brechtel, F. J., Russell, L. M., Weber, R. J., Gras, J., Hudson, J. G. and Litchy, M. 1997. Intercomparison study of size dependent counting efficiency of 26 condensation particle counters. *Aerosol Sci. and Technol.* **27**, 224–242.

Wood, R., Johnson, D., Osborne, S., Andreae, M. O., Bandy, B., Bates, T. S., O'Dowd, C. Glantz, P., Noone, K., Quinn, P. K., Rudolph, J. and Suhre, K. 2000. Boundary layer and aerosol evolution during the third Lagrangian experiment of ACE-2. *Tellus* **52B**, 401–422.